Hydrogen Bonding in Supercritical Ethanol Assessed by Infrared and Raman Spectroscopies

P. Lalanne, J. M. Andanson, J.-C. Soetens,* T. Tassaing, Y. Danten, and M. Besnard

Laboratoire de Physico-Chimie Moléculaire, UMR 5803 CNRS-Université Bordeaux I 351, Cours de la Libération, 33405 Talence Cedex, France

Received: July 31, 2003

This present paper is aimed at discussing the state of aggregation in supercritical ethanol using infrared and Raman spectroscopies. A quantitative band shape analysis of the spectra associated with the OH stretching mode of ethanol has been done using IR and Raman activities determined by ab initio calculations on small oligomers. Such a methodology allows the quantification of the degree of hydrogen bonding (η), and both IR and Raman techniques lead to comparable results. This study shows that hydrogen bonds still exist in supercritical ethanol. The degree of hydrogen bonding (η) is found to be relatively constant above the critical density and strongly diminishes below it. The determined values of η are consistent with literature measurements reported using IR spectroscopy. The disagreement observed with NMR experiments has been critically discussed.

1. Introduction

Since the early 1960s, the state of aggregation of alcohols in the liquid state has been the subject of numerous experimental and theoretical investigations.[1,2] Indeed, detailed knowledge about the structure and dynamics in self-associated liquids, such as alcohols, is of crucial importance for the understanding of the hydrogen bond interaction. For this purpose, the methodology generally adopted was to investigate solutions of alcohol dissolved in inert solvents at room temperature. The progressive evolution of the state of molecular aggregation on going from the monomeric form of alcohol toward the building of the H bond network in neat liquids has been assessed by the increase of the alcohol concentration in the mixture.[3−8] In pure alcohols, investigations have been reported in a moderate temperature range (vicinity of the boiling point) and with pressures from 0.1 to 100 MPa.[9,10] More recently, studies on H bonds have been extended to supercritical fluids (SCFs).[11−13] Indeed, under these thermodynamic conditions, the density of the fluid can be varied continuously from gaslike to liquidlike values. Thus, the tuning of the density of the fluid provides a nice route toward a deeper insight about the assessment of this specific intermolecular interaction. Besides fundamental studies, supercritical fluids are of importance in industrial applications (extraction processes, material science). In particular, supercritical water is often used as solvent because the value of the dielectric constant can be continuously tuned over a wide density range.[14] Again, supercritical alcohols constitute an alternative for the use of SC water not only since critical conditions are less extreme but also since the dielectric constant remains relatively high, ensuring good solvating properties. Moreover, methanol and ethanol are widely used as cosolvents in a number of industrial processes (fractionation, extraction, etc.) in order to enhance the solubility of polar and high molecular weight solutes in supercritical CO_2.[15,16]

Experimental and theoretical studies devoted to the structure and dynamics of pure alcohols in the supercritical state are scarce. The NMR investigations carried out by Hoffman and Conradi,[13] Bai and Yonker,[17] and Asahi and Nakamura[18] were aimed at evaluating the degree of hydrogen bonding in supercritical alcohols as a function of the temperature and the pressure. These authors have pointed out that hydrogen bonding was still existing in the supercritical domain even at high temperatures. As a matter of fact, the degree of hydrogen bonding reported by Hoffman and Conradi[13] was found to be about 30% of that in liquid methanol and ethanol at room temperature. Incidentally, it was also found that hydrogen bonded aggregates of alcohol molecules already exist at low gaslike densities. A study of supercritical methanol by neutron diffraction carried out by Yamaguchi et al.[19] showed that the number of hydrogen bonds decreases as the temperature and pressure increase. At constant density ($\rho \sim 0.786$ g cm^{-3}) at the temperatures $T = 513$ and 526 K in the pressure range 14 MPa $< P <$ 24.5 MPa, the authors report that methanol molecules are aggregated to form clusters involving five or six hydrogen bonds. Finally, a study of supercritical methanol performed by Raman scattering[20] led also to the conclusion of the existence of hydrogen bonded molecules under supercritical conditions.

From the theoretical point of view, Chalaris and Samios[21] have carried out a molecular dynamics simulation of supercritical methanol. Their results are in good agreement with the NMR experiments and thus confirm their conclusions. In addition, they have been able to determine the percentage distribution of hydrogen bonds per molecule, giving a more quantitative picture of the state of aggregation in liquid and supercritical methanol.

The present paper is aimed at providing insights about the state of aggregation of neat ethanol in the supercritical state using vibrational spectroscopies. For this purpose, we have selected the OH stretching vibration of the molecule which is known to be a very sensitive probe of the hydrogen bonding phenomena. We have performed this investigation using infrared absorption and Raman scattering.

This choice has been guided by the fact that the activities of the OH mode in hydrogen bonded clusters of alcohols markedly differ in these spectroscopic techniques. In infrared spectroscopy, the activity of the OH oscillator involved in an hydrogen bond

10.1021/jp0309466 CCC: $27.50

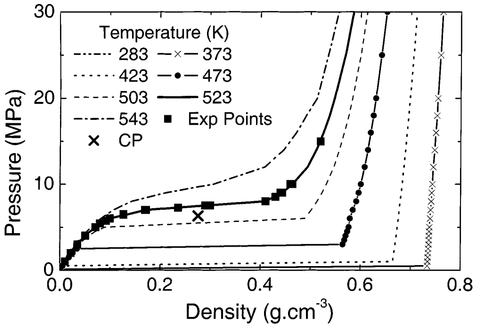

Figure 1. Phase diagram of ethanol. The state points investigated along the isotherm $T = 523$ K are displayed by full squares and the critical point ($P_c = 6.4$ MPa, $T_c = 516$ K, $\rho_c = 0.28$ g cm^{-3}) is displayed by a bold times sign.

is greatly enhanced compared with that associated with “free” hydroxyl groups. Moreover, this enhancement is generally higher for OH groups involved in larger aggregates. However, in Raman spectroscopy, the activities of the free and bonded OH modes are not so drastically different and weakly depend on the cluster size. Comparison of these two complementary techniques is certainly the way to come to consistent and well grounded conclusions concerning the state of aggregation of alcohols. As far as we know, this approach has not been fully undertaken in investigations of H bonds in SCFs, which have been mostly studied by IR absorption. The interpretation and quantitative analysis of the vibrational spectra have been carried out using ab initio calculations. From the calculated dipole moment derivatives (in infrared absorption) and the polarizability derivatives (in Raman) of the free and hydrogen bonded OH stretching modes of ethanol species, we have been able to determine the relative distribution of the various oligomers present in the fluid as a function of density.

2. Experimental Details

2.1. Thermodynamic States. The phase diagram of ethanol obtained from thermodynamic data[22] reported in the literature is displayed in Figure 1. This figure illustrates the advantage of working under supercritical conditions, as discussed in the Introduction. Modest pressure and temperature variations in the vicinity of the critical point allow one to perform measurements of the vibrational spectra in a continuous way in a broad density domain varying by about 1 order of magnitude from liquidlike to gaslike densities. We have performed the measurements in the supercritical domain, under isothermal conditions at a temperature of 523 K for densities ranging between 0.01 and 0.6 g cm^{-3} (see Figure 1). We have also undertaken experiments at ambient conditions to compare with the results obtained under supercritical conditions. Absolute ethanol used in this study was provided by Prolabo (99.9% purity) and used without further purification.

2.2. Midinfrared Spectroscopy. The measurements were performed on a Biorad interferometer (type FTS-60A) equipped with a globar source, a silicon beam splitter supported on a KBr plate, and a DTGS detector. Single beam spectra recorded in the spectral range 400−6000 cm^{-1} with a 2 cm^{-1} resolution were obtained by the Fourier transformation of 100 accumulated interferograms. We have used a special stainless steel cell designed in our laboratory in order to obtain a thin film of ethanol at high temperatures up to 513 K and under pressures of up to 15 MPa. The sealing of the cell was ensured by a Viton O-ring which was disposed around the window. The cell was equipped with sapphire windows separated with a copper spacer, ensuring a path length of 15 μm. The heating of the cell was performed using a band heater disposed around the cell in which two thermocouples were placed. The first one was located close to the band heater to achieve temperature control, and the second was kept close to the sample area in order to ensure good temperature regulation with an accuracy of about ±2 K. The cell was connected via a stainless steel capillary to a manual pump (Top Industrie SA), allowing pressures of up to 50 MPa to be reached with an absolute uncertainty of ±0.1 MPa and a relative error of ±0.3%.

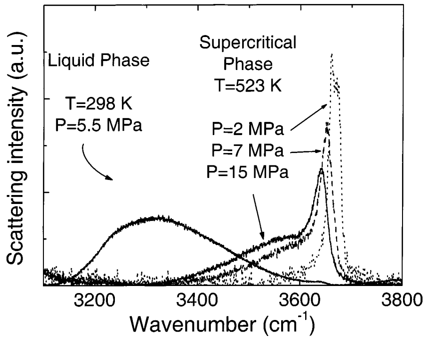

Figure 2. Comparison of the polarized $I_{VV}(\nu)$ Raman spectra in the OH stretching region of liquid and supercritical ethanol.

2.3. Raman Spectroscopy. The Raman spectra were measured using a DILORS (Z24) triple-monochromator spectrometer equipped with a photomultiplier detector. The source was a Spectra Physics Krypton ion laser operating at a wavelength of 647.1 nm with a power of 600 mW. The polarized $I_{VV}(\bar{\nu})$ spectra were recorded in the spectral range 2800−3800 cm^{-1} with a resolution of 0.6 cm^{-1} using the standard 90° scattering geometry. To obtain a good signal-to-noise ratio, each spectrum required a time of accumulation of about 60 min. The Raman stainless steel cell (316L) used had four windows. Two silica windows each were used for the entrance of the laser beam and for the detection of the scattered light, respectively. Silica, which is optically isotropic, has been used to minimize shear induced birefringence effects, thus ensuring a proper polarization observation of the incident and scattered electric field of the laser light. The other windows were made in sapphire and respectively used for the exit of the laser beam and to allow a visual observation of the fluid contained in the cell. The windows had a diameter of 12 mm and a thickness of 5 mm. The sealing was obtained using the unsupported area principle. All windows were positioned on the flat surface of the inconel plug with a 100 μm thick gold foil placed between the window and the plug in order to compensate for imperfections at the two surfaces. Flat copper seals were used to ensure a proper sealing between the plug and the body cell. The heating of the cell was achieved by four cartridge heaters placed directly into the body of the cell. The temperature and the pressure were controlled as explained previously for the infrared measurements. This setup allowed temperatures and pressures of about 573 K and 40 MPa to be reached.

3. Experimental Results

3.1. Raman Scattering. The polarized $I_{VV}(\bar{\nu})$ Raman spectra associated with the OH stretching vibration of pure supercritical ethanol at the constant temperature $T = 523$ K and pressures of 2, 7, and 15 MPa are displayed in Figure 2. The spectrum of liquid ethanol at 298 K and 5.5 MPa is also reported for comparison on this figure. In liquid ethanol, the broad band observed in the spectral range 3100−3600 cm^{-1} is assigned to OH bonded groups of the hydrogen bond *donor* molecules

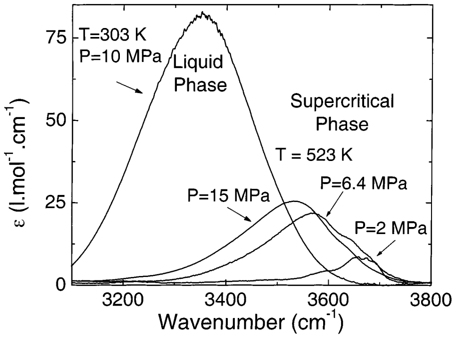

Figure 3. Comparison of the infrared spectra of liquid and supercritical ethanol in the OH stretching region.

(which may be simultaneously acceptor molecules) of ethanol oligomers. The very weak band observed at ~3640 cm^{-1} is associated with the free OH stretching mode of monomeric ethanol and the hydrogen bond *acceptor* molecules at the end of the open chain oligomers.[5,23] The band center frequencies of these two free OH modes are too close to be resolved here. Thus, in the liquid state, ethanol molecules are primarily hydrogen bonded and only very few molecules should exist under monomeric form.

In marked contrast, in the high temperature gaseous phase at low density ($P = 2$ MPa), the Raman spectrum exhibits only a single band centered at ~3650 cm^{-1} which clearly shows that mostly ethanol monomers exist under these conditions. In the supercritical domain, we observe an intermediate situation between the two previous extreme cases. Indeed, the broad band associated with the alcohol network has disappeared and the spectrum is now composed of a broad band situated at ~3550 cm^{-1} accompanied by a narrow and intense profile at ~3630 cm^{-1}. The former is assigned to the OH bonded groups of the hydrogen bond *donor* molecules of small ethanol oligomers, whereas the latter is associated with free OH stretching modes of both monomeric ethanol and the hydrogen bond *acceptor* molecules. These results show that a dramatic redistribution of the state of aggregation takes place upon going from the liquid phase to the SCF. In the SC state, as the pressure is increased from 7 to 15 MPa (from $\rho \sim 0.1$ to 0.5 g/cm^3), the overall Raman band shape remains similar. However, we see (Figure 2) that the free OH band is red-shifted and broadened. The same trend, although less apparent, seems to be followed by the band associated with oligomers. Clearly, under isothermal conditions, a large increase in the density (from 0.1 to 0.5 g/cm^3) has little effect on the state of aggregation of the ethanol molecules. The previous finding might suggest that increasing the density slightly favors oligomeric forms in the equilibrium between small aggregates and monomers. The evolution of these spectra is significant and clearly shows that large H bonded oligomers[10] observed in the liquid state have been broken in the SC domain, leading to the formation of small aggregates, and monomers as well, of ethanol.

3.2. Infrared Absorption. We have reported in Figure 3 the infrared spectra of the OH stretching mode of ethanol in the supercritical state at the temperature $T = 523$ K and at pressures ranging from 2 to 15 MPa. The spectrum measured for liquid ethanol at 303 K and 10 MPa is also displayed on this figure for comparison. In the liquid phase, we observe again a broad band between 3100 and 3600 cm^{-1} assigned to the hydrogen bonded OH groups. In contrast with the case of Raman spectroscopy, the very weak feature associated with the free OH stretching mode of ethanol molecules is not detected now. This finding shows that all the ethanol molecules are hydrogen bonded to form a network. In the SC domain at $P = 15$ MPa, we observe again a broad band situated however between 3300 and 3800 cm^{-1} which is now assigned to the H bonded OH stretching modes in the aggregates of ethanol. However, the integrated intensity, the frequency position of the band center, and the band shape are dependent upon the fluid density. At the density $\rho \sim 0.1$ g cm^{-3} ($P \sim 6.4$ MPa), the spectrum exhibits two shoulders respectively situated at ~3675 and 3648 cm^{-1} in the spectral range of the non-H bonded OH vibration. A comparison with the IR spectrum of gaseous ethanol at $P = 2$ MPa shows that these shoulders are remnants of the PQR type spectral structure (Figure 3). These findings allow us to assign the two previous shoulders to the OH stretching vibration of monomers of ethanol. As the density is increased up to $\rho \sim 0.5$ g cm^{-3} ($P \sim 15$ MPa), these shoulders disappear and the profile is red-shifted with an enhanced intensity. From all these results, we may infer that SC ethanol is only constituted by small aggregates at this density value.

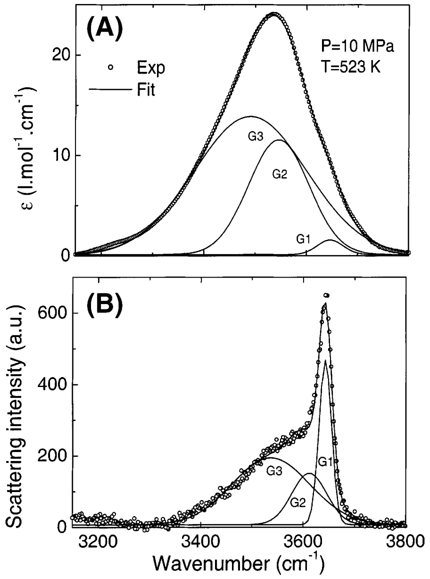

Figure 4. Decomposition of the infrared (A) and Raman (B) spectra of supercritical ethanol at $T = 523$ K and $P = 10$ MPa using a weighted sum of Gaussian profiles.

3.3. Conclusion. From Raman and infrared measurements, it clearly appears that the H bond network existing in liquid ethanol is broken under SC conditions, leading to a fluid in which only small oligomers subsist under the experimental conditions investigated. It is also noteworthy that the spectral signature of the free OH groups is particularly marked in Raman scattering, whereas the bonded OH stretching modes of small aggregates of ethanol are observed in infrared absorption.

4. Quantitative Analysis

4.1. Preliminary Discussion. A quantitative analysis of the band shape can be performed from a decomposition of the spectra as a weighted sum of Gaussian profiles. The best fit was achieved using three components for both Raman and infrared spectra. The first component (G1) (see Figure 4) is associated with the free OH stretching mode, and the two others are related to the contribution due to the small aggregates (G2 and G3). In the treatment of the infrared spectra, the band center frequency of the Gaussian profile for the free OH stretching mode was fixed to that obtained from the fit of the Raman spectra. This procedure is justified by the fact that in Raman spectra the free OH feature is clearly observed. Incidentally, let us emphasize that the decomposition of the band shape using

Lorentzian profiles does not allow one to obtain a fit with the quality obtained from the Gaussian decomposition. This result indicates that the frequency distribution of the OH stretching mode of ethanol molecules is inhomogeneous, even at the highest temperature investigated here. Such inhomogeneous distribution has also been observed for water oligomers at high temperature.[24] On the grounds of the preceding discussion, we may assign the first Gaussian profile to the free OH stretching modes of both monomeric ethanol and the hydrogen bond *acceptor* molecules at the ends of open chain oligomers, whereas the two other components might be attributed to bonded OH groups of the hydrogen bond *donor* molecules at the internal positions of ethanol oligomers. On the basis of these preliminary results, we made the hypothesis that G2 and G3 might be respectively associated with dimers and trimers and larger hydrogen bonded clusters are expected to be in much lower proportion. Although this preliminary analysis specifies the nature of the species existing in the SC fluid, it does not allow one to determine their respective concentrations. Indeed, the intensity of a spectral transition associated with a specific species is given by the product of the concentration of this species and the transition dipole moment in absorption studies or the transition polarizability in Raman studies. Thus, the determination of the population from this spectral decomposition requires one to know the values of the transition moments associated with the free and hydrogen bonded OH stretching modes in the different ethanol oligomers. For this purpose, we have performed ab initio calculations, which are presented in the following section.

4.2. Ab Initio Calculations. In this section, we report the results of ab initio calculations carried out on clusters of ethanol molecules, namely, the monomer, dimer, and cyclic and linear trimers. In the electronic ground state, ethanol presents one trans conformer (C_s point group) and two mirror-image gauche conformers (C_1 point group). A recent ab initio study revisited the potential energy surface of the molecule[25] and found that the two conformers are nearly isoenergetic (energy difference of 18.8 cm^{-1}) and interconvert through the torsion of the hydroxyl group with an energy barrier of 404 cm^{-1}. These values are in excellent agreement with spectroscopic studies.[26,27] This result suggests that under our experimental conditions all the possible conformers for ethanol molecules are involved in dimers and trimers. Nevertheless, the frequencies and intensities of the OH stretching modes are comparable for the two conformers in monomers; therefore, we only considered the trans conformation. The previously published[28,29] ab initio studies on ethanol clusters were mainly devoted to structural and energetic properties. George et al.[4] reported frequencies and IR intensities for clusters of up to four ethanol molecules in order to analyze the IR spectra of dilute solutions in CCl_4. Recently, in a study of different hydrogen bonding complexes,[30] it has been suggested that a high level of computations (at least MP2/cc-pV5Z) is necessary to describe accurately the intermolecular interaction energies in these systems. As we want to apply the present methodology to large alcohol molecules involved in clusters, we have determined in the case of methanol through various levels of calculation (up to MP2/cc-pV5Z) that the MP2/6-31G* level is a good compromise between computational cost and quality of results in terms of relative intensities (i.e., ratio of free and bonded OH activities). In this context, we have carried out calculations for the trans conformation of ethanol at the MP2/6-31G* level using the Gaussian 98 program.[31] Full structure optimizations were performed and used to evaluate harmonic frequencies and infrared and Raman intensities. The optimized structures of the trans ethanol monomer, dimer, and cyclic and linear trimers are shown on Figure 5, and the computed values are reported in Tables 1 and 2. The calculated infrared and Raman intensities and frequencies associated with the OH stretching modes of the ethanol monomer, dimer, and trimers (cyclic and linear) are reported in Figure 6 together with the typical experimental spectra for SC ethanol at $T = 523$ K and $P = 7.5$ MPa.

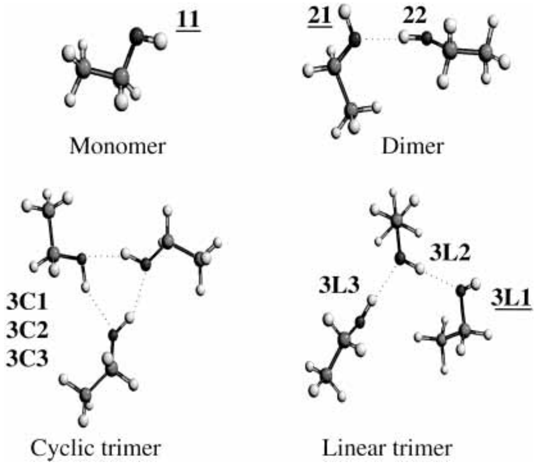

Figure 5. MP2/6-31G* optimized geometries of the ethanol monomer, dimer, and trimers.

TABLE 1: Total Energies (E), Binding Energies (ΔE_{CP}), and Average Bond Energies per Number of H Bonds ($\Delta E_{\mathrm{CP}}/N_{\mathrm{H\ bonds}}$)

		E (au)	ΔE_{CP}* (kJ/mol)	$\Delta E_{\mathrm{CP}}/N_{\mathrm{H\ bonds}}$ (kJ/mol)
C_2H_5OH	trans	−154.516970		
	gauche	−154.517122		
$(C_2H_5OH)_2$		−309.048390	−21.3	−21.3
	d	−154.520331		
	a	−154.519926		
$(C_2H_5OH)_3$	cyclic	−463.591156	−67.7	−22.6
	da	−154.521859		
	da	−154.521769		
	da	−154.521749		
$(C_2H_5OH)_3$	linear	−463.585122	−54.4	−27.2
	a	−154.520562		
	da	−154.521979		
	d	−154.521877		

As expected from previous spectroscopic investigation on ethanol clusters in the gas phase[32] and in the liquid phase,[6] we observe a decrease in the calculated frequencies of the OH stretching mode from the monomer to the trimers. Nevertheless, the values of the intensities and the frequencies of the free OH stretching mode are found to be very close for all the species. In addition, we observe a strong growth in the infrared intensities of the hydrogen bonded OH mode of aggregates of increasing size (up to 40 times that of the free OH mode), whereas the corresponding Raman activities remain at about the same order of magnitude (not exceeding 3.1 times that of the free OH mode) (see Table 2). This corroborates the difference between the infrared and Raman band shapes, as discussed in section 3.

4.3. Spectral Analysis. *Methodology.* We have considered that the fluid is composed of an assembly of p_1 monomers, p_2 dimers, and p_3 trimers, and we have associated with the transition of the OH stretches of ethanol in each species a Gaussian profile. In addition, the Gaussian profile is weighted by the computed Raman or infrared intensities of the corresponding stretching OH mode. We have considered a model to fit our experimental spectra involving monomers, dimers, and

TABLE 2: Scaled Harmonic Frequencies, IR Intensities, Raman Intensities, and Depolarization Ratios (ρ_{depol}) for the OH Stretching Mode Obtained from Ab Initio Calculations on Ethanol Clusters[a]

		mode label	freq (cm^{-1})		IR (km/mol)		Raman (A^4/amu)		ρ_{depol}
(C_2H_5OH)	trans	11	3779	(0)	21.89	(1.0)	96.62	(1.0)	0.30
	gauche		3770		18.21		60.93		0.28
(C_2H_5OH)$_2$	d	22	3653	(−126)	422.56	(19.3)	155.49	(1.6)	0.29
	a	21	3771	(−8)	35.01	(1.6)	88.44	(0.9)	0.31
(C_2H_5OH)$_3$	cyclic	3C1	3542	(−237)	809.24	(37.0)	76.24	(0.8)	0.75
		3C2	3538	(−241)	891.12	(40.7)	83.43	(0.9)	0.75
		3C3	3456	(−323)	4.84	(0.2)	296.53	(3.1)	0.11
(C_2H_5OH)$_3$	linear	3L1	3765	(−14)	38.46	(1.8)	86.64	(0.9)	0.29
		3L2	3584	(−195)	538.40	(24.6)	97.85	(1.0)	0.69
		3L3	3529	(−250)	673.30	(30.8)	178.38	(1.8)	0.13

[a] Values in parentheses are the frequency shifts and the relative intensities with respect to the free OH stretching mode obtained for the monomer, respectively, at the same level of calculation.

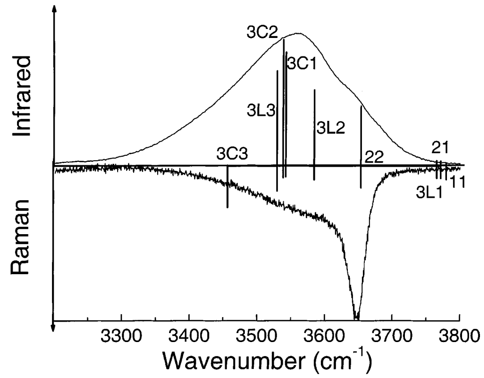

Figure 6. Ab initio results on infrared and Raman intensities and band center frequencies as compared with the experimental spectra of supercritical ethanol at $T = 523$ K and $P = 7.5$ MPa.

cyclic and/or *linear* trimers. It is noteworthy that we have also tested models in which only *cyclic* trimers or *linear* trimers are involved. Only the general model led to a consistent analysis of the IR and Raman profiles and will be discussed below.

We gathered the OH transitions in six classes, namely (11, 21, 3L1); (22); (3C1, 3C2); (3L2); (3L3); and (3C3) (see Figure 5 for notation), according to the fact that the spectroscopic intensities and frequencies are similar within the same class. We can also notice that all the free OH groups belong to the same class (the first class). This grouping enables us to greatly reduce the number of parameters involved in the fitting procedure. To go further into the analysis and to lead to a more tractable fitting treatment, we assumed that, within the same class, the Gaussian profiles associated with each OH transition have the same parameters (band center frequency and width) and are weighted by a factor defined as the product of the population and the intensity of each respective OH mode.

The decomposition of the profile is expressed as

$$S(\bar{\nu}) = (p_1a_{11} + p_2a_{21} + p_{3L}a_{3L1})g_{\text{class 1}}(\bar{\nu}) + (p_2a_{22})g_{\text{class 2}}(\bar{\nu}) + (p_{3C}a_{3C1} + p_{3C}a_{3C2})g_{\text{class 3}}(\bar{\nu}) + (p_{3L}a_{3L2})g_{\text{class 4}}(\bar{\nu}) + (p_{3L}a_{3L3})g_{\text{class 5}}(\bar{\nu}) + (p_{3C}a_{3C3})g_{\text{class 6}}(\bar{\nu})$$

where p_i is the population of the cluster of size i, a_{ij} is the Raman or infrared intensity of the OH mode labeled ij (see Table 2), and g_{ij} denotes the Gaussian profile defined by

$$g_{\text{class }i}(\bar{\nu}) = \frac{1}{\sigma_i\sqrt{\pi/2}} \exp\left\{-2\left(\frac{\bar{\nu} - \bar{\nu}_i}{\sigma_i}\right)^2\right\}$$

where σ_i is the full width at half-height and $\bar{\nu}_i$ is the band center frequency (whose fitted values are reported in Table 3).

TABLE 3: Fitted Parameters of the Gaussian Deconvolution of the Infrared and Raman Spectra of Supercritical Ethanol at $T = 523$ K and $P = 6.0$ and 8.0 MPa

	fit results			
	infrared		Raman	
	$P = 6.0$ MPa	$P = 8.0$ MPa	$P = 6.0$ MPa	$P = 8.0$ MPa
p_1	0.8073	0	4.4532	0.0211
p_2	0.0363	0.0387	0.2045	2.1715
p_{3C}	0	0.1306	0.9752	1.7353
p_{3L}	0.3047	0.3969	0	0.3395
$\bar{\nu}_1$	3676.3	3667.7	3661.0	3651.6
σ_1	39.1	43.6	21.6	19.3
$\bar{\nu}_2$	3644.4	3637.6	3632.3	3644.0
σ_2	27.1	35.9	17.2	39.5
$\bar{\nu}_3$		3521.0	3616.5	3587.6
σ_3		134.0	85.86	92.3
$\bar{\nu}_4$				3532.0
σ_4				135.0
$\bar{\nu}_5$	3517.7	3454.4		3603.3
σ_5	174.0	181.1		50.0
$\bar{\nu}_6$	3586.2	3568.3	3595.1	3606.1
σ_6	95.9	103.0	28.7	53.7
% free OH	64.0	26.2	59.8	23.9
% bonded OH	36.0	73.8	40.2	76.1
% monomer	45.0	0	57.2	0.2
% dimer	4.0	4.7	5.3	41.0
% trimer	51.0	95.3	37.6	58.8

Within the same class, the fitted parameters are the frequency ($\bar{\nu}_i$), the fwhh (σ_i), and p_i. Raman or infrared intensities are fixed at their computed ab initio a_{ij} values (cf. Table 2).

This model has been tested on the experimental spectra at two thermodynamic state points, namely, at $P = 6$ and 8 MPa and $T = 523$ K. A typical decomposition of the experimental profiles is displayed in Figure 7. A good agreement between the experimental and calculated profiles has been obtained in the infrared and Raman spectroscopies for the three models. Fitted parameters for the previous examples are presented in Table 3. The first result is that, independently of the model used, the values of the band center frequencies of the profiles associated with the five classes of OH oscillators are found to follow the hierarchy $\bar{\nu}_1 > \bar{\nu}_2 > \bar{\nu}_3 > \bar{\nu}_4, \bar{\nu}_5, \bar{\nu}_6$, in accordance with the ab initio predictions.

We have computed the percentages of free and hydrogen bonded OH groups, respectively defined by

$$P_{free} = (p_1 + p_2 + p_{3L})/(p_1 + 2p_2 + 3p_{3L} + 3p_{3C})$$

$$P_{bonded} = 1 - P_{free}$$

where p_1, p_2, p_{3L}, and p_{3C} are the populations associated with the monomer, dimer, linear trimer, and cyclic trimer of ethanol,

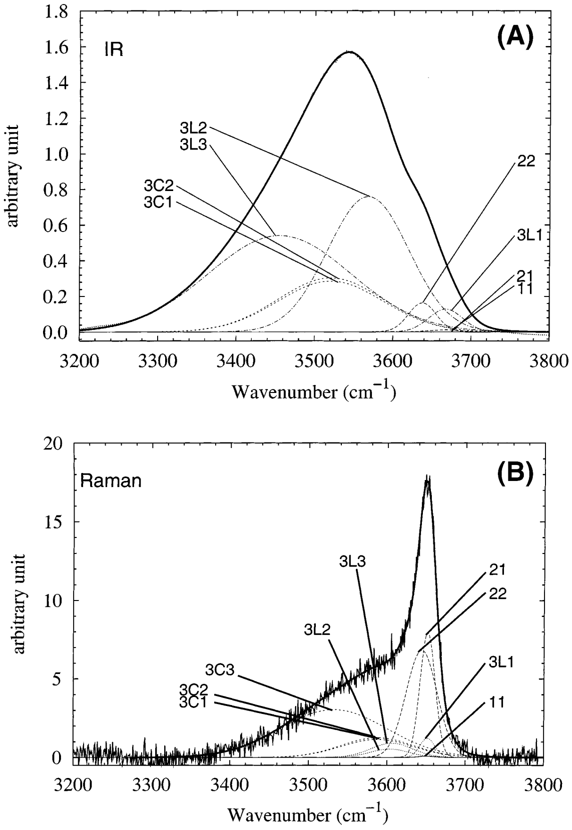

Figure 7. Decomposition of the infrared (A) and Raman (B) spectra of supercritical ethanol at $T = 523$ K and $P = 7.0$ MPa, according to the model (see text).

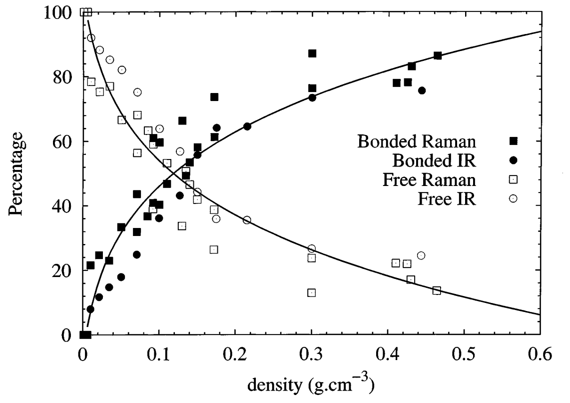

Figure 8. Evolution of the percentage of free and hydrogen bonded OH in supercritical ethanol as a function of density at constant temperature $T = 523$ K.

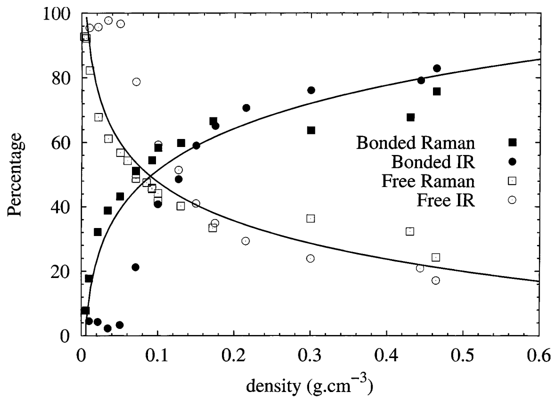

Figure 9. Comparison of the evolution of the percentage of free OH bonded ethanol molecules with the density using our model and the data treatment proposed by Barlow et al.[11]

respectively. These quantities have been calculated from the populations (p_i) and are reported in Table 3.

5. Results and Discussion

The evolution as a function of density of the percentages of free and hydrogen bonded OH groups is reported on Figure 8. We observe a good agreement between the infrared and Raman results over the whole range of densities, which confirms that the general model used for the decomposition is well suited for the analysis of the present data. It comes out that, at high densities, the percentage of free OH is rather low, as 80% of the OH groups of ethanol molecules are hydrogen bonded. This percentage is nearly constant at densities higher than the critical density. However, at densities below $\rho = 0.2$ g cm^{-3}, a strong increase in the percentage of the free OH groups up to 60% is observed. Thus, we conclude that the degree of hydrogen bonding in supercritical ethanol strongly increases with the density beyond the critical density. It is noteworthy that the evolution of the population of ethanol oligomers remains almost similar using models involving either cyclic or linear trimers.

5.1. Comparison with Other Vibrational Spectroscopic Investigations. Recently, an investigation of hydrogen bonding in a series of liquid SC alcohols[11] has been carried out by IR spectroscopy to evaluate the fraction of hydrogen bonded and non-hydrogen bonded hydroxyl groups as a function of both temperature and pressure. An original approach for the analysis of the ν(OH) spectra has been proposed which can be used when density data are lacking and/or the path length of the cell is not available. The method involves the following steps. The ν(OH) profiles measured at different temperatures and pressures, normalized by the intensities of the corresponding ν_s(CH) bands associated with the methyl groups, are decomposed into spectra associated with bonded and nonbonded (the so-called monomeric) species. The evolution with the pressure of the integrated intensity (I_{nb}) of the monomeric band is then extrapolated to zero pressure by fitting an exponential function to get the integrated intensity coefficient (A_{nb}) of the monomeric group. This yields the mole fraction of the non-H bonded OH groups as $X_{nb} = I_{nb}/A_{nb}$, with the mole fraction of the H bonded groups as $X_b = 1 - X_{nb}$. Though this procedure is rather difficult for small molecules, the authors have succeeded in evaluating the degree of hydrogen bonding (η) in SC ethanol at 350 °C. We have applied their approach to our spectroscopic measurements. The analysis of the infrared and Raman spectra has allowed us to evaluate the percentage of free OH bonds, reported on Figure 9. Clearly, a nice agreement between this approach and our results combining IR and Raman data with ab initio calculations is observed. Several conclusions can be drawn from this agreement.

The procedure proposed in the literature to treat the experimental data to get the percentage X_{nb} is valid for both IR and Raman data, and it is noteworthy that this procedure is independent of any clustering model. The consistency obtained between our results and the literature data using the same type of analysis reinforces the reliability of the experimental data obtained in the different laboratories. As a consequence, we are rather confident in the theoretical analysis proposed here which leads to a partition scheme of SC ethanol involving three species. Let us emphasize that this conclusion cannot be reached from the simple procedure of the literature. We can therefore safely conclude that vibrational spectroscopy leads to a consistent picture of the state of aggregation in SC ethanol between bonded and nonbonded species.

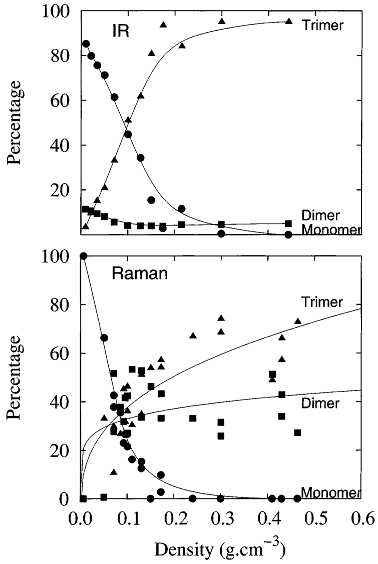

Figure 10. Evolution of the calculated percentage of ethanol molecules involved in monomers, dimers, and trimers in SC ethanol as a function of the density along the isotherm $T = 523$ K.

According to the consistency of the vibrational spectroscopic investigations, we can precisely evaluate the evolution of the state of aggregation in SC ethanol using our model. Examination of Figure 10 shows that the diminution of hydrogen bonding can be interpreted as a strong increase in the monomer population at the expenses of the trimers as the density decreases. The percentage of monomers which is close to zero at high densities increases up to 80−100% at low densities, whereas the percentage of trimers which is about 80% at high densities decreases nearly to zero at low densities. Finally, the percentage of dimers is found to be between 10 and 30% and nearly independent of the density.

5.2. Comparison with Other Techniques and Discussion. At this point, we have to compare the results obtained by vibrational spectroscopy with currently available information provided by other spectroscopic techniques and MD simulations. This can be done upon a comparison of the average number of hydrogen bonds per ethanol molecule (n_{HB}).

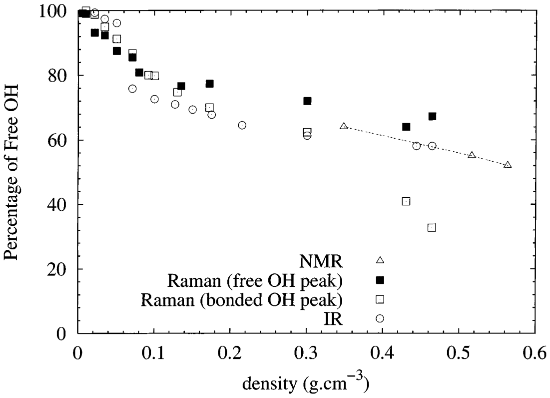

Figure 11. Comparison of the evolution of the percentage of free OH bonded ethanol molecules with the density obtained from NMR chemical shifts[13] with those obtained from our IR and Raman data based upon the dichotomic model (see text section 5.2). In the case of the Raman spectra, the dichotomic model has been applied to both free and "bonded" OH peaks. In the case of the infrared spectra, this is restricted to the bonded component, as the maximum of the free contribution is not observed.

Various definitions of this quantity have been used in previous studies, and we must precisely state this definition. In MD simulations,[7] an ethanol molecule is considered to be hydrogen bonded to another one according to a geometric and/or an energetic criterion, independent of whether or not the molecule is the donor (D) or the acceptor (A). Therefore, in solid alcohol, where each molecule is involved in two hydrogen bonds as the donor and the acceptor, the previous definition leads to an average number of hydrogen bonds per ethanol molecule of $n_{HB}{}^{(DA)} = 2$. For liquid ethanol under ambient conditions, this number is found to be equal to 1.9.[7] For liquid methanol, which has been studied under various thermodynamic conditions, this number is found to be equal to 1.9[7] and 1.85[21] under ambient conditions and typically decreases down to 0.7−0.9 in dense supercritical methanol at $T = 523$ K and $P = 10{-}20$ MPa.[21] The same quantity has been derived by Yamaguchi et al.[19] for supercritical methanol using a combined neutron scattering and empirical potential structure refinement. It was found that $n_{HB}{}^{(DA)} = 1.77$ under ambient conditions and 1 in dense supercritical methanol at $T = 526$ K and $P = 14.3$ MPa. Hoffman and Conradi[13] have proposed to derive the degree of hydrogen bonding (η) from the evolution of the NMR chemical shift of the hydroxyl protons of methanol and ethanol as a function of temperature and pressure. They have employed a dichotomic two-state model (i.e., alcohol molecules are either H bonded or not) to quantify the extent of hydrogen bonding using the room temperature liquid as an arbitrary reference state. Under the hypothesis of the fast exchange limit between the two forms, the observed chemical shift is then the concentration weighted average of the two types of hydroxyl proton shifts. It turns out that the extent of hydrogen bonding (η) present in the alcohols is linearly related to the shift, with a value equal to 1 for the room temperature liquid and to 0 for the zero density limit.

Their calculated average number of hydrogen bonds given per ethanol molecule ($n_{HB}{}^{(D)}$) is related to the degree of hydrogen bonding (η) by $n_{HB}{}^{(D)} = 0.925\eta$. The normalization factor, 0.925, is defined as half the value of $n_{HB}{}^{(DA)} = 1.85$ of liquid methanol, with $n_{HB}{}^{(DA)} = 2n_{HB}{}^{(D)}$. We have reported the percentages of free hydrogen bonded OH groups from the value of $n_{HB}{}^{(D)}$ taken from the NMR measurements on Figure 11. In the density range 0.35−0.6, the values of this percentage continuously decrease from 65 to 55%. Clearly, if we compare the NMR data with our vibrational spectroscopic results displayed in Figures 8 and 9, the values markedly differ between the two techniques. To interpret this difference, we have used the approach proposed in NMR studies to treat the infrared and Raman data. We have assumed that the dichotomic model used in NMR studies is valid. We emphasize at this point that the observation time in vibrational spectroscopy is in the picosecond range, and therefore, in contrast to the NMR spectra, the spectra of free and bonded species are resolved (i.e., the slow exchange limit condition applies this time). This allows us to discuss the band shifts corresponding to the NMR chemical shifts for free and bonded species. Taking the room temperature liquid as a reference state and assuming a linear evolution of the shift, we have calculated the percentage of free OH from the H bonded component obtained from the decomposition of the infrared and Raman spectra. The comparison of the results of this calculation with the NMR data (Figure 11) clearly shows that a good agreement between the different techniques is obtained.

This result is puzzling because we do know that the population from which the previous percentage is derived requires a further analysis of vibrational spectra taking into account the transition moments.

Therefore, we believe that the agreement obtained between the different techniques is rather dubious. Indeed, it is implicitly assumed in the previous treatment that the shift evolution relates two physical situations which are in fact different. It is somehow postulated that the H bond network observed in the liquid evolves continuously to lead to the monomeric form. We have experimentally shown before that the passage from aggregated species toward a H bond network is a complex process. It seems likely that the simple extrapolation procedure used here is able to capture the essence of this physical process. This can be appreciated by performing the same type of analysis on the shift of the free OH component observed in Raman. We found again a nice agreement between the evolution with the density of the percentage of free species obtained from this analysis and that obtained from the data treatment proposed by Barlow et al. (Figure 9). It is surprising to assume that the shift of the free OH band is related to the evolution of the percentage of the free species (where is the network in this case?) instead of being an environmental effect.

Finally, we come to the conclusion that the approach based upon the band shifts analyzed using a dichotomic model, taking the room temperature liquid as a standard for 100% of H bonded species, is a gross approach whose usefulness is to provide a way to compare results of different techniques but without deep theoretical grounding. We also conclude that hydrogen bonds still exist in supercritical ethanol in which monomers and small aggregates, namely dimers and trimers, are present.

Acknowledgment. This work was performed under the auspices of the “programme pluri-formation n° 971022” entitled “Etude spectroscopique de fluides dans le domaine supercritique” from the University of Bordeaux I.

References and Notes

(1) Joesten, M. D.; Schaad, L. J. *Hydrogen Bonding*; Marcel Dekker: New York, 1974.

(2) Pimentel, G. C.; McClellan, A. L. *The Hydrogen Bond*; Reinhold Publishing Corp.: New York, 1960.

(3) Liddel, U.; Becker, E. D. *Spectrochim. Acta* **1957**, *10*, 70.

(4) George, W. O.; Has, T.; Hossain, M. F.; Jones, B. J.; Lewis, R. *J. Chem. Soc., Faraday Trans.* **1998**, *94*, 2701.

(5) Woutersen, S.; Emmerichs, U.; Bakker, H. J. *J. Chem. Phys.* **1997**, *107*, 1483.

(6) Laenen, R.; Rauscher, C. *J. Chem. Phys.* **1997**, *107*, 9759.

(7) Padro, J. A.; Saiz, L.; Guardia, E. *J. Mol. Struct.* **1997**, *416*, 243.

(8) Staib, A. *J. Chem. Phys.* **1998**, *108*, 4554.

(9) Fishman, E.; Drickamer, J. *J. Chem. Phys.* **1956**, *24*, 548.

(10) Perchard, C.; Perchard, J. P. *J. Raman Spectrosc.* **1978**, *7*, 173.

(11) Barlow, S. J.; Bondarenko, G. V.; Gorbaty, Y. E.; Yamaguchi, T.; Poliakoff, M. *J. Phys. Chem. A* **2002**, *106*, 10452.

(12) Bulgarevich, D. S.; Otake, K.; Sako, T.; Sugeta, T.; Takebayashi, Y.; Kamizawa, C.; Shintani, D.; Negishi, A.; Tsurumi, C. *J. Chem. Phys.* **2002**, *116*, 1995.

(13) Hoffman, M. M.; Conradi, M. S. *J. Phys. Chem. B* **1998**, *102*, 263.

(14) Shaw, R. W.; Brill, B.; Clifford, A.; Eckert, A.; Franck, E. U. *Chem. Eng. News* **1991**, *69*, 26.

(15) Rey, S.; Cansell, F. *Polym. J.* **1998**, *30*, 863.

(16) Tassaing, T.; Lalanne, P.; Rey, S.; Cansell, F.; Besnard, M. *Ind. Eng. Chem. Res.* **2000**, *39*, 4470.

(17) Bai, S.; Yonker, C. R. *J. Phys. Chem. A* **1998**, *102*, 8641.

(18) Asahi, N.; Nakamura, Y. *J. Chem. Phys.* **1998**, *109*, 9879.

(19) Yamaguchi, T.; Benmore, C. J.; Soper, A. K. *J. Chem. Phys.* **2000**, *112*, 8976.

(20) Ebukoro, T.; Takami, A.; Oshima, Y.; Koda, S. *J. Supercrit. Fluids* **1999**, *15*, 73.

(21) Chalaris, M.; Samios, J. *J. Phys. Chem. B* **1999**, *103*, 1161.

(22) Vargaftik, N. B. *Tables on the thermophysical properties of liquids and gases*; John Wiley: New York, 1975.

(23) Graener, H.; Ye, T. Q.; Laubereau, A. *J. Chem. Phys.* **1989**, *90*, 3413.

(24) Carey, D. M.; Korenowski, G. M. *J. Chem. Phys.* **1998**, *108*, 2669.

(25) Senent, M. L.; Smeyers, Y. G.; Dominguez-Gomez, R.; Villa, M. *J. Chem. Phys.* **2000**, *112*, 5809.

(26) Durig, J. R.; Larsen, R. A. *J. Mol. Struct.* **1990**, *238*, 195.

(27) Pearson, J. C.; Sastry, K.; Herbst, E.; De Lucia, F. C. *J. Mol. Spectrosc.* **1996**, *175*, 246.

(28) Huelsekopf, M.; Ludwig, R. *J. Mol. Liq.* **2000**, *85*, 105.

(29) Sum, A. K.; Sandler, S. I. *J. Phys. Chem. A* **2000**, *104*, 1121.

(30) Tsuzuki, S.; Uchimaru, T.; Matsumura, K.; Mikami, M.; Tanabe, K. *J. Chem. Phys.* **1999**, *110*, 11906.

(31) Frisch, M. J.; Trucks, G. W.; Schlegel, H. B.; Gill, P. M. W.; Johnson, B. G.; Robb, M. A.; Cheeseman, J. R.; Keith, T.; Peterson, G. A.; Montgomery, J. A.; Raghavachari, K.; Al-Laham, M. A.; Zakrewski, V. G.; Ortiz, J. V.; Foresman, J. B.; Ciolowski, J.; Stefanov, B. B.; Nanayakkara, A.; Challacombe, M.; Peng, C. U.; Ayala, P. Y.; Chen, W.; Wong, M. W.; Andres, J. L.; Replogle, E. S.; Comperts, R.; Martin, R. L.; Fox, D. J.; Binkley, J. S.; DeFrees, D. J.; Baker, J.; Steward, J. J. P.; Head-Gordon, M.; Gonzalez, C.; Pople, J. A. *Gaussian 98*; Gaussian, Inc.: Pittsburgh, PA, 1994.

(32) Haber, T.; Schmitt, U.; Suhm, M. A. *Phys. Chem. Chem. Phys.* **1999**, *1*, 5573.